

Available online at www.sciencedirect.com

ScienceDirect

www.elsevier.com/locate/jes

JES
 JOURNAL OF
 ENVIRONMENTAL
 SCIENCES
www.jesc.ac.cn

Insight into the adsorption of tetracycline onto amino and amino-Fe³⁺ functionalized mesoporous silica: Effect of functionalized groups

Ziyang Zhang¹, Haiyan Li^{1,*}, Huijuan Liu²

1. Beijing Engineering Research Center of Sustainable Urban Sewage System Construction and Risk Control, Beijing University of Civil Engineering and Architecture, Beijing 100044, China. E-mail: zhangziyang@bucea.edu.cn

2. Key Laboratory of Drinking Water Science and Technology, Research Center for Eco-Environmental Sciences, Chinese Academy of Sciences, Beijing 100085, China

ARTICLE INFO

Article history:

Received 7 August 2016

Revised 13 October 2016

Accepted 26 October 2016

Available online 18 March 2017

Keywords:

Adsorption

Mesoporous silica

Amino groups

Fe³⁺

Tetracycline

ABSTRACT

In order to study the influences of functionalized groups onto the adsorption of tetracycline, we prepared a series of amino and amino-Fe³⁺ complex mesoporous silica adsorbents with diverse content of amino and Fe³⁺ groups (named N,N-SBA15 and Fe-N,N-SBA15). The resulting mesoporous silica adsorbents were fully characterized by X-ray powder diffraction (XRD), Fourier transform infrared spectrometer (FTIR) and N₂ adsorption/desorption isotherms. Furthermore, the effects of functionalized groups on the removal of TC were investigated. The results showed that the periodic ordered structure of SBA-15 was maintained after modification of amino/Fe³⁺ groups. The functionalized amino groups decreased the adsorption capacity while the coordinated Fe³⁺ increased the adsorption capacity. The adsorption kinetics of TC fitted pseudo-second-order model well and the equilibrium was achieved quickly. The adsorption isotherms fitted the Langmuir model well and with the Fe³⁺ content increased from 3.93% to 8.26%, the Q_{max} of the adsorbents increased from 102 to 188 mmol/kg. The solution pH affected the adsorption of TC onto amino complex adsorbents slightly while influenced the adsorption onto Fe-amine complex adsorbents greatly. The adsorption of TC on SBA15 and N,N-SBA15 may be related to the formation of outer-sphere surface complexes, while the adsorption of TC onto Fe-N,N-SBA15 was mainly attributed to the inner-sphere surface complexes. This study could offer potential materials that have excellent adsorption behavior for environmental remediation and suggested useful information for the preparing other adsorbents in environmental applications.

© 2017 The Research Center for Eco-Environmental Sciences, Chinese Academy of Sciences.

Published by Elsevier B.V.

Introduction

Tetracycline-antibiotics, one of the most antibiotics, are used worldwide in controlling the infection from both humans and animals. Furthermore, tetracycline-antibiotics are also used for agricultural purpose and animal growth promoter (Ötöker

and Akmeahmet-Balcioğlu, 2005; Kim et al., 2010). However, most of tetracycline-antibiotics are poorly absorbed by human and animals after intake, about 25%–75% of added compounds are excreted or released as metabolite forms into environment via feces or urine (Chee-Sanford et al., 2001). Tetracycline (TC), the second most widely used antibiotics in the world (Yu et al.,

* Corresponding author. E-mail: lihaiyan@bucea.edu.cn (Haiyan Li).

2009; Luo et al., 2011), like other tetracycline-antibiotics, is difficult to be degraded because of the main structure-naphthol ring. The mass used tetracycline-antibiotics make the large amount TC residue into environment. As serious environmental pollution, TC residue in the environment induces resistant microorganisms and brings a threat to the human health (Xu and Li, 2010; Gu et al., 2007). Recently, residues of TC are frequently detected in sewage, agricultural wastewater, surface water, groundwater and even drinking water (Chen et al., 2014; Chen and Zhou, 2014; Tong et al., 2014; Tang et al., 2015). However, natural biodegradation and conventional water treatment are not effectual for the removal of TC from aqueous solution (Ji et al., 2009; Lv et al., 2015). Therefore, great attentions have been focused on the developing efficient technologies for TC removal.

Recently, many methods have been used for removing TC from aqueous solution, such as oxidation, photo-catalysis, membrane separation, biodegradation and adsorption (Zazouli et al., 2009; Zhao et al., 2010; Wang et al., 2015; Chang and Ren, 2015; Alvarez-Torrellas et al., 2016). Compared with other methods, adsorption has received increasing attention due to the lower total cost, higher efficiency and friendliness (Dai et al., 2014). Many adsorbents such as soils, clays, activated carbon, graphite and mesoporous silica are used to remove TC from aqueous solution (Ji et al., 2009; Sassman and Lee, 2005; Figueroa et al., 2004; Ahmed et al., 2015). Among these adsorbents, ordered mesoporous silica has got great interest because of its high surface area, large pore volume, controllable pore size and stable aqueous dispersion (Puanngam and Unob, 2008). However, due to the abundant silanol groups present on the channel walls, the mesoporous silicates have lower adsorption capacities for antibiotics. Therefore, introduction of the functional groups on the mesoporous silica surface and framework was created to enhance the adsorption property (Bui and Choi, 2009; Rivera-Jimenez et al., 2010; Vu et al., 2010a, 2010b). Accordingly, amino and Fe groups were successfully functionalized to control the antibiotics delivery and increase the adsorption capacity, separately (Rivera-Jimenez et al., 2010; Wu et al., 2013). In recent years, some researchers have prepared amino/Fe functionalized mesoporous silica by first grafting amino groups and then coordinating Fe, and investigated the adsorption behavior for removal of pollutants from aqueous solutions (Zuo et al., 2012). Our previous study confirmed that amino-Fe functionalized SBA15 has high adsorption efficiency for TC due to the complexation between Fe and TC (Zhang et al., 2015a, 2015b). To the best of our knowledge, the interaction between functionalized groups (amino and Fe) and TC was not clear, especially the coexisting of them on the surface of mesoporous silica.

In this article, diverse content of functionalized groups was introduced on mesoporous silica SBA15 and the influences of groups on the removal of TC were investigated. The characteristics of prepared materials have been thoroughly evaluated by X-ray powder diffraction (XRD), Fourier transform infrared spectrometer (FTIR) and N_2 adsorption/desorption isotherms. The influence of amino and Fe^{3+} groups on the adsorption properties was also investigated by kinetic and isotherm measurements. Furthermore, batch experiments were carried out to study the fundamental adsorption behavior at different pH and ionic strength/species.

1. Methods and materials

1.1. Reagents

Tetraethyl orthosilicate (TEOS, 98%) and Pluronic P123 (PEO20PPO70PEO20, $M_w = 5800$) were obtained from Alfa Aesar Corp. The hydrochloride salt of TC was obtained from Sigma Co. and used without further purification. Toluene, acetonitrile, methanol, isopropanol high performance liquid chromatography (HPLC grade) and 3-(2-aminoethylamino)-propyltrimethoxysilane were purchased from Alfa Aesar Corp, all other chemicals were analytical grade. Water with a resistivity greater than $18.2 M\Omega/cm$ (Milli-Q) was used for all experiments.

1.2. Synthesis of amino/ Fe^{3+} incorporated mesoporous silica

SBA15 was prepared by using TEOS as the silica source and pluronic P123 as the templating reagent (Wu et al., 2013). Amino-incorporation SBA15 was synthesized by a step-wise fashion using grafting techniques. First, 1.5 g SBA-15 was prepared at $120^\circ C$, *in vacuo* for 2 hr, then the prepared materials were suspended in 150 mL of anhydrous toluene and stirred for approximately 1 hr under a dry N_2 flow. Next, diverse amount of 3-(2-aminoethylamino)-propyltrimethoxysilane was added and the mixture was stirred under reflux at $100^\circ C$ for 24 hr under a dry N_2 flow. The products were filtered, washed with dry toluene and isopropanol consecutively. Finally, the samples were dried overnight named as N,N-SBA15 (N1, N2, N3). Fe^{3+} -amine complex SBA15 was prepared by immobilized Fe^{3+} onto N,N-SBA15. One gram (1.0 g) samples were mixed with a 0.1 mol/L isopropanol solution of ferric trichloride for 24 hr. The mixture was filtered, washed with isopropanol and dried overnight named Fe-N,N-SBA15 (FeN1, FeN2, FeN3). To investigate the influence of dosage of 3-(2-aminoethylamino)-propyltrimethoxysilane and ferric trichloride onto the adsorption process, different contents of amino/ Fe^{3+} adsorbents were prepared by changing the proportion of 3-(2-aminoethylamino)-propyltrimethoxysilane and ferric trichloride.

1.3. Characterization of adsorbents

The synthesized samples were characterized by XRD patterns using a X'pert PRO-MPD diffractometer (Panlitical, Holland). All XRD patterns were collected in the 2θ range between 0.5 and 3° with a scanning rate of $0.01^\circ/min$. The textural properties of the samples were measured via nitrogen adsorption-desorption isotherms at $-196^\circ C$ (77 K) using a Micromeritics ASAP2020HD88 (Mike, USA). Fourier transform infrared spectrometer was obtained in a Tenson 27 FTIR Spectrometer (Bruker, Germany) via KBr pellet method. Powder samples were analyzed at $4/cm$ resolution an averaged over 400 scans in the absorption band range of $4000-400/cm$. The elemental analysis was conducted on a Vario ELIII (Elementar, Germany). The sorbent was digested with acid mixture of hydrogen nitrate-perchloric acid-hydrofluoric acid compound (5:4:5, V/V/V) by the constant temperature electric heating plate, and Fe^{3+} content was determined by an inductively coupled plasma optical emission spectrometer (ICP-OES) (Elan 5000, Perkin Elmer, USA). The zeta potential

was measured using a Nano Particle Sizing & Zeta potential Analyzer (Beckman Coulter, U.S.A).

1.4. Adsorption experiments

All batch experiments were conducted in the dark to inhibit the potential photo-degradation of TC. To elucidate the function of amino and Fe^{3+} groups in the adsorption process, SBA15, N,N-SBA15 and Fe-N,N-SBA15 were used to study the adsorption properties using kinetic and isotherm measurements. The kinetic adsorption studies were investigated by adding 0.5 g adsorbents into 500 mL solutions with the initial TC concentration of 0.1 mmol/L. The mixture was shaken with a speed of 150 r/min at $25 \pm 1^\circ\text{C}$. Hydrochloric acid and sodium hydroxide were used to adjust the solution pH to 5.0 ± 0.1 . At different time intervals, the samples were collected and filtrated through a $0.45 \mu\text{m}$ membrane filter for the determined of TC concentration.

Adsorption isotherms experiments of TC on the adsorbents were carried out by adding 0.05 g adsorbents to 50 mL solutions containing TC at 0, 0.01, 0.03, 0.05, 0.07, 0.1, 0.15 and 0.2 mmol/L. The solution pH was adjusted to 5.0 ± 0.1 with hydrochloric acid and sodium hydroxide. The mixture was shaken with a speed of 150 r/min at $25 \pm 1^\circ\text{C}$ for 24 hr to reach equilibrium. Finally, the mixture was filtrated through a $0.45 \mu\text{m}$ membrane filter and the concentration of TC in the solution was analyzed.

To further investigate amino/ Fe^{3+} group on the adsorption of TC, SBA15, N1, FeN1 were used in the experiments on pH effect. The experiments were conducted by adding a mass of 0.05 g adsorbents into 50 mL solutions containing TC at the initial concentration of 0.1 mmol/L. The solution pH was adjusted to different values between 3 to 9 using hydrochloric acid and sodium hydroxide. Other experimental conditions were the same as mentioned in adsorption isotherms.

To investigate the effect of ionic strength and ion species on the adsorption of TC, SBA15, N1, and FeN1 were used in the experiments. The experiments were conducted by adding a mass of 0.05 g adsorbent into 50 mL solutions containing TC at the initial concentration of 0.1 mmol/L with different ionic strengths (1, 100 mmol/L) and ion species (Na^+ , K^+ , Ca^{2+} , CO_3^{2-} , SO_4^{2-} , NO_3^-). The solution pH was adjusted to 5.0 ± 0.1 with hydrochloric acid and sodium hydroxide. Other experimental conditions were the same as mentioned in adsorption isotherms.

The TC concentrations were determined by a HPLC (Agilent 1260, USA) at a wavelength of 360 nm. The mobile phase was a mixture of 0.01 mmol/L oxalic acid–acetonitrile–methanol (67:22:11, V/V) at a flow rate of 1 mL/min.

2. Results and discussions

2.1. Characterization of the synthesized adsorbents

The mass composition of C, H, N and Fe of adsorbents was showed in Table 1. After the modification of functionalized groups, the presence of N and Fe provided an evidence for the successful incorporation of the organic groups and Fe^{3+} on the adsorbents. Furthermore, the content of N and Fe on the samples was different with different dosages of 3-(2-aminoethylamino)-propyltrimethoxysilane and ferric trichloride. The amino groups

Table 1 – Elemental analysis data of samples.

		N%	C%	H%	Fe%
SBA-15		0.04	1.07	0.85	0.03
N,N-SBA15	N1	2.43	11.02	2.06	0.01
	N2	3.22	12.06	2.26	0.02
	N3	4.19	15.28	2.71	0.03
Fe-N,N-SBA15	FeN1	2.24	11.28	1.78	3.93
	FeN2	2.67	12.20	2.20	5.09
	FeN3	3.25	13.70	2.44	8.26

on the SBA15 influenced the Fe% greatly, with the mass composition of N increased from 2.43% to 4.19%, the mass composition of Fe increased from 3.93% to 8.26%. The original SBA15 has a specific surface area of $492.03 \text{ m}^2/\text{g}$, an average pore diameter of 6.5 nm and a pore volume of $0.82 \text{ cm}^3/\text{g}$. After amino functionalization, the surface area, average pore diameter and pore volume of N3 sample decreased to $282.69 \text{ m}^2/\text{g}$, 6.46 nm and $0.55 \text{ cm}^3/\text{g}$, respectively. Furthermore, after the incorporation of Fe^{3+} , the parameters of FeN3 sample decreased further with the value of $245.29 \text{ m}^2/\text{g}$, 6.12 nm and $0.38 \text{ cm}^3/\text{g}$.

Fig. 1 shows the low-angle XRD pattern of SBA15, N,N-SBA15 and Fe-N,N-SBA15 with diverse content of functionalized groups. SBA15 exhibits three well defined X-ray diffraction peaks at 0.9 , 1.6 and 1.9° , which can be indexed to the dominant reflection peak (100), (110) and (200), suggesting a p6mm symmetry-typical of uniform mesopore structure with two-dimension (2D) hexagonal long-range order (Zhao et al., 1998; Garg et al., 2008). After amino modification, all the XRD patterns of N,N-SBA15 showed the peaks of d100, d110 and d200, which demonstrated that periodic ordered structure of SBA-15 was maintained. However, with the increasing content of amino group, the diffraction intensity decreased and the position of peaks changed, which revealed some extent of disorder, especially for the diffraction peak of d110 and d200. These results suggested that the amino groups had successful incorporated into the pore walls of SBA15. After the incorporation of Fe^{3+} , the diffraction intensity of three peaks decreased further and the latter two reflections nearly disappeared, which

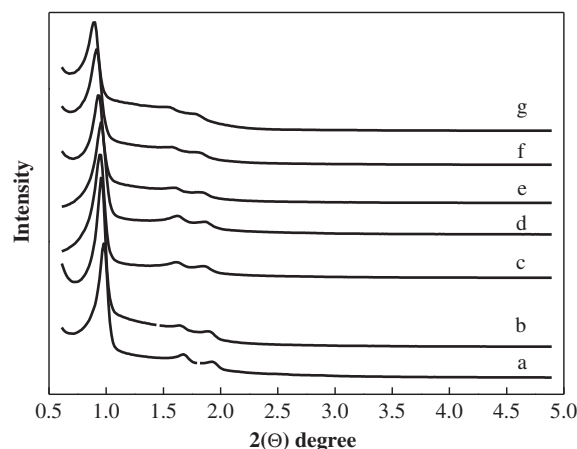


Fig. 1 – Low-angle XRD pattern of SBA15, N,N-SBA15 and Fe-N,N-SBA15. Line a: SBA15; line b: N1; line c: FeN1; line d: N2; line e: FeN2, f-N3; line g: FeN3. XRD: X-ray powder diffraction.

confirmed the presence of Fe^{3+} in the pore walls. Furthermore, with the content of functionalized Fe^{3+} increased, the peak of d100 shifted to the lower degree.

The FTIR spectra of SBA15, N,N-SBA15 and Fe-N,N-SBA15 with diverse content of functionalized groups are shown in Fig. 2. For SBA-15, the bands at 808, 1077, 3398 and 961/cm may be attributed to the symmetric vibrations, asymmetric vibrations of Si–O–Si, and the stretching vibrations and symmetric vibrations of Si–OH, respectively. After grafting amino groups, new weak bands appear at 2937 and 1463/cm, which may be attributed to the stretching vibrations of N–H, vibrations of $-\text{CH}_2$ and symmetric vibrations of N–H respectively (Oh et al., 2007; Lam et al., 2007), indicating the anchoring of the amino group. Furthermore, with the content of amino groups increasing, the intensity of these vibrations increased obviously. After the incorporation of Fe^{3+} , all the N–H vibrations shifted to the lower wavelength, which demonstrated that the chemical environment of amino groups was changed by the coordination of Fe^{3+} . All the results were consistent with the analysis in Table 1 and Fig. 1.

2.2. Adsorption kinetics of TC onto the sorbents

Fig. 3 shows the adsorption kinetics of TC onto SBA15, N,N-SBA15 and Fe-N,N-SBA15. Most of TC were adsorbed rapidly onto the adsorbents first, followed by a relatively slow process. The adsorption rate followed the order of N,N-SBA15 > SBA15 > Fe-N,N-SBA15. Compared with the adsorption kinetic of SBA15, the adsorption process onto N,N-SBA15 nearly belongs to the same model, indicating that the diverse content of amino groups did not affect the adsorption mechanism. The same results were found in the adsorption kinetics of Fe-N,N-SBA15. The rapid adsorption rate for all adsorbents could be induced by the high surface area, large pore volume and controllable pore size, which enhanced the internal mass transfer in the adsorption process. Furthermore, compared with SBA15, the amino groups inhibited the adsorption of TC onto the sorbents. With the content of amino group increased the adsorption capacity of TC decreased slightly. On the contrast,

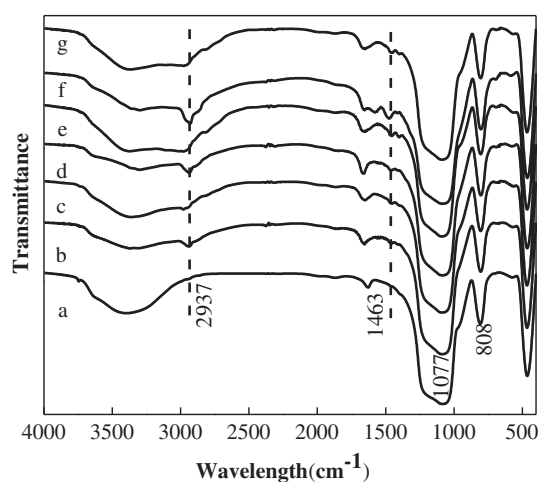


Fig. 2 – The fourier transform infrared spectroscopy (FTIR) of SBA15, N,N-SBA15 and Fe-N,N-SBA15. Line a: SBA15; line b: N1; line c: FeN1; line d: N2; line e: FeN2, f-N3; line g: FeN3.

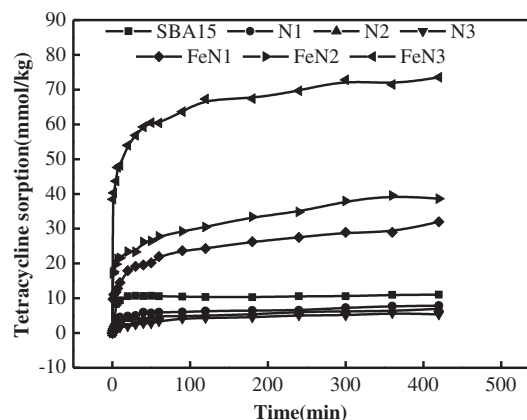


Fig. 3 – Adsorption kinetics of TC onto SBA15, N,N-SBA15 and Fe-N,N-SBA15. Experimental conditions: $[\text{TC}]_0 = 0.1 \text{ mmol/L}$, $m = 1 \text{ g/L}$, $\text{pH} = 5.0 \pm 0.1$, $T = 25^\circ\text{C}$. TC: tetracycline.

with the mass composition of Fe^{3+} increasing, the adsorption capacity of TC onto the mesoporous silica increased greatly.

To investigate the adsorption of TC onto the mesoporous silica further, the adsorption kinetics of TC data were analyzed using pseudo-first-order and pseudo-second-order models which are listed below as Eqs. (1) and (2) (Wang et al., 2007):

$$\ln(Q_e - Q_t) = \ln Q_e - k_1 t \quad (1)$$

$$\frac{t}{Q_t} = \frac{1}{k_2 Q_e^2} + \frac{t}{Q_e} \quad (2)$$

where, Q_t (mmol/kg) is the amount of TC adsorbed at time t (min), and Q_e (mmol/kg) represents the amount of TC adsorption at equilibrium, k_1 (min^{-1}) and k_2 ($\text{kg}/\text{mmol}/\text{min}$) were the rate constants of the pseudo-first-order and pseudo-second-order, respectively.

The calculated parameters and correlations results are listed in Table 2. As the correlation coefficients showed, two models were well consistent with the adsorption process of TC onto the sorbents. Compared with the pseudo-first-order model, the pseudo-second-order model had higher correlation coefficients ($R^2 > 0.99$). The experimental and calculated values of Q_e were very close, suggesting that the pseudo-second-order model was more suitable for describing the sorption progress of TC onto the sorbents.

2.3. Adsorption isotherms of TC onto the sorbents

To investigate the influences of functionalized groups on the adsorption of TC further, the adsorption isotherms of TC onto the sorbents are shown in Fig. 4. The amount of TC adsorbed on the sorbents increased with increasing equilibrium concentration. Compared with SBA15, the instillation amino groups would decrease the adsorption capacity of TC onto mesoporous silica. While, the incorporation of Fe^{3+} would provide large amount of useful adsorption site and enhanced the removal of TC from aqueous solutions. With the mass composition of Fe^{3+} increased, the adsorption capacity of TC increased significantly. The adsorption isotherms of

Table 2 – Parameters and correlation coefficients of pseudo-first-order and pseudo-second-order.

	Pseudo-first-order			Pseudo-second-order		
	Q _e (mmol/kg)	K ₁ (min ⁻¹)	R ²	Q _e (mmol/kg)	K ₂ (g/(mg·min))	R ²
SBA15	7.46	0.013	0.88	10.80	0.0039	0.99
N1	6.02	0.012	0.89	8.26	0.0042	0.98
N2	5.36	0.013	0.90	7.85	0.0048	0.98
N3	4.87	0.012	0.95	5.78	0.0056	0.97
FeN1	18.82	0.0082	0.95	31.87	0.0020	0.99
FeN2	21.83	0.0097	0.93	38.69	0.0019	0.99
FeN3	30.82	0.0114	0.92	73.69	0.0019	0.99

N,N-SBA15 and Fe-N,N-SBA15 show the same model, indicating that the diversity of functionalized groups did not affect adsorption mechanism. These results were consistent with the analysis in the adsorption kinetics of TC onto adsorbents.

To investigate the adsorption isotherms further, the Langmuir and Freundlich models were used to represent the behavior of adsorption TC onto mesoporous silica. The Langmuir and Freundlich models are presented in Eqs. (3) and (4), respectively.

$$Q_e = \frac{Q_{max} b C_e}{1 + b C_e} \tag{3}$$

$$Q_e = K_f C_e^{1/n} \tag{4}$$

where, C_e is the initial and equilibrium concentration of TC (mmol/L), Q_{max} (mmol/kg) is the maximum adsorption capacity, b is a measure of the energy of adsorption, K_f is the Freundlich adsorption constant and n is related to the adsorption intensity.

Langmuir isotherm based on the assumption that the adsorbate is attributed in the homogenous surface and there is no interaction between the adsorbate molecules. Freundlich isotherm based on the adsorption happened on a heterogeneous surface. The parameters and coefficients of the two models are shown in Table 3. Compared with the Freundlich model, the Langmuir isotherm (R² = 0.92–0.98) was more suitable for describing the adsorption progress, illustrating that the adsorption process was single molecule layer adsorption. The Q_{max}

of the adsorbents followed as FeN3 > FeN2 > FeN1 > SBA15 > N1 > N2 > N3. These results were consistent with the conclusion in the adsorption kinetics, the presence of amino groups and Fe³⁺ influenced the adsorption behavior significantly. With the N% increased from 0.03% to 4.19%, the Q_{max} of the adsorbents decreased from 41.11 to 26.41 mmol/kg. However, after the coordination of Fe³⁺ onto the pore channel of mesoporous silica, the adsorption capacity of TC was enhanced obviously. With the content of Fe³⁺ increased from 0% to 8.26%, the Q_{max} increased from 41.11 to 188.74 mmol/kg. Compared with SBA15 and N,N-SBA15, the incorporation of Fe³⁺ onto the surface of the adsorbent could offer abundant sorption sites for TC removal. Furthermore, n calculated from Freundlich is a constant indicative of adsorption intensity or surface heterogeneity. Table 3 shows that the values of n were less than 10 for all samples, indicating that the adsorption of TC onto the sorbents was favorable, especially for the Fe-N,N-SBA15.

2.4. The effect of pH on the adsorption of TC

To investigate the adsorption of TC further, the effect of solution pH on the adsorption process of SBA15, N1 and FeN1 is shown in Fig. 5. Compared with SBA15, the incorporation of amino groups decreased the adsorption capacity in nearly all pH values. While, after the grafting of Fe³⁺ group onto N,N-SBA15, the adsorption capacity increased greatly, though the Fe³⁺ content was only 3.93%. These results were consistent with the conclusion of adsorption kinetics and isotherms. As shown in Fig. 6, the charge of SBA15 is mainly negative in all pH values. After the incorporation of amino group, the zeta potential increased greatly. The amino group on the surface of SBA15 could offer abundant useful site for the Fe³⁺ incorporation. The incorporation of Fe³⁺ increased the charge of the sorbents further. The high adsorption capacity may be

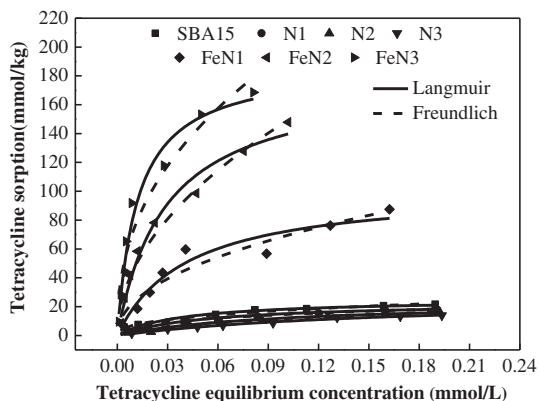


Fig. 4 – Adsorption isotherms of TC onto SBA15, N,N-SBA15 and Fe-N,N-SBA15. Experimental conditions: [TC]₀ = 0–0.2 mmol/L, m = 1 g/L, pH = 5.0 ± 0.1, T = 25°C. TC: tetracycline.

Table 3 – Parameters and correlation of adsorption isotherms of tetracycline on the sorbents.

	Langmuir			Freundlich		
	Q _{max} (mmol/kg)	L	R ²	K _f (mmol ¹⁻ⁿ L ⁻ⁿ .kg)	n	R ²
SBA15	41.11	20.58	0.92	41.96	2.63	0.93
N1	35.26	18.02	0.93	33.63	2.75	0.84
N2	28.45	10.25	0.96	30.25	1.93	0.98
N3	26.41	5.80	0.98	8.35	1.44	0.91
FeN1	102.11	23.94	0.93	202.22	2.14	0.91
FeN2	179.35	34.58	0.98	470.27	1.99	0.97
FeN3	188.74	81.49	0.96	515.50	2.37	0.93

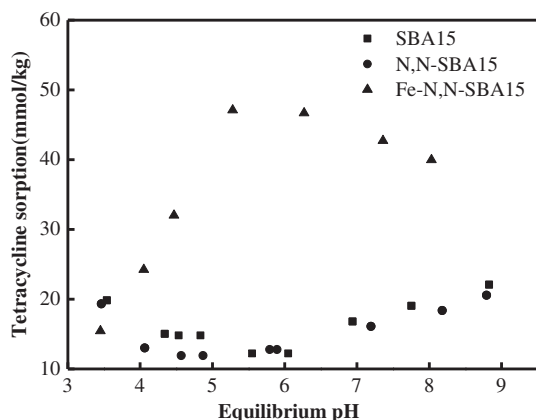


Fig. 5 – The effect of pH on the adsorption of TC onto SBA15, N,N-SBA15 and Fe-N,N-SBA15. Experimental conditions: $[TC]_0 = 0.1$ mmol/L, $m = 1$ g/L, $T = 25^\circ\text{C}$. TC: tetracycline.

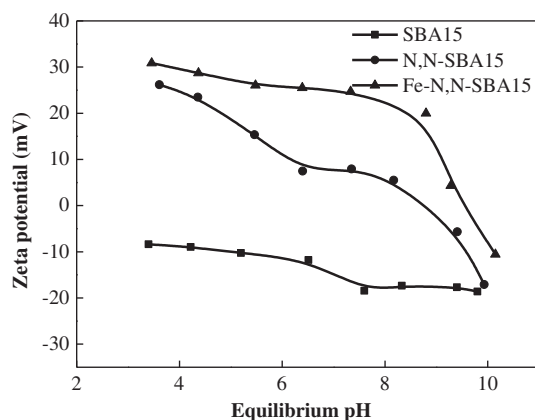


Fig. 6 – Zeta potential of SBA15, N,N-SBA15 and Fe-N,N-SBA15.

attributed the amount of activate site on the surface of SBA15 caused by the incorporation of Fe^{3+} .

For SBA15 and N,N-SBA15, with the solution pH increasing, the adsorption of TC first decreased slightly and then increased.

For Fe-N,N-SBA15, with the solution pH increasing, the effect of pH could be divided into three regions: the adsorption increased when $\text{pH} < 5.0$, stayed nearly unchanged when pH is in the range of 5–7; and decreased dramatically when pH increased further. The speciation of adsorbate in aqueous solution and the surface chemistry of the adsorbent may play an important role in the adsorption process. With the solution pH increasing, the TC species and the charge of the adsorbents changed. TC is an amphoteric molecule having multiple ionizable functional groups Fig. 7a and forms a series of species when the solution pH changes Fig. 7b. The predominate TC (symbolized as H_2L) species are H_3L^+ at $\text{pH} < 3.4$, H_2L at $3.4 < \text{pH} < 7.6$, HL^- at $7.6 < \text{pH} < 9.0$, and L^{2-} at $\text{pH} > 9.0$ (Kang et al., 2010). For SBA15 and N,N-SBA15, with the pH increasing from acidic to neutral, the adsorption capacity decreased may be attributed to the electrostatic repulsion caused by the deprotonation of the tricarbonylamide, suggested that the electrostatic interactions may play an important role in the adsorption process. The adsorption capacity increased at $\text{pH} > 6$ may be attributed to the interaction of phenolic diketone group and the adsorbents. For Fe-N,N-SBA15, in acidic to neutral conditions, the deprotonation of the tricarbonylamide group could interact with the Fe^{3+} (Figuroa and Mackay, 2005; Zhao et al., 2014). Furthermore, the electrostatic attraction between TC and adsorbent increased and enhanced the adsorption capacity. When pH is in $5 < \text{pH} < 7$, the phenolic diketone group of TC started to deprotonate, and served as the group involved in complexation with the adsorbent surface. The adsorption capacity decreased at $\text{pH} > 7$ may be attributed to the unfavorable electrostatic conditions between TC molecules and Fe-N,N-SBA15 surfaces.

2.5. Effect of ionic strength and ion species on the adsorption of TC

The influence of ionic strength and ion species on TC adsorption was investigated and the results are shown in Fig. 8. Three kinds of anion and cation were chosen to investigate the influence caused by the natural aqueous solution. For SBA15 and N,N-SBA15, the results showed that all the ion species have little effect on the adsorption of TC when the ionic strength was 1 mmol/L. However, with the ionic strength increased to 100 mmol/L, the adsorption capacity decreased greatly. For Fe-N,N-SBA15, with the ionic

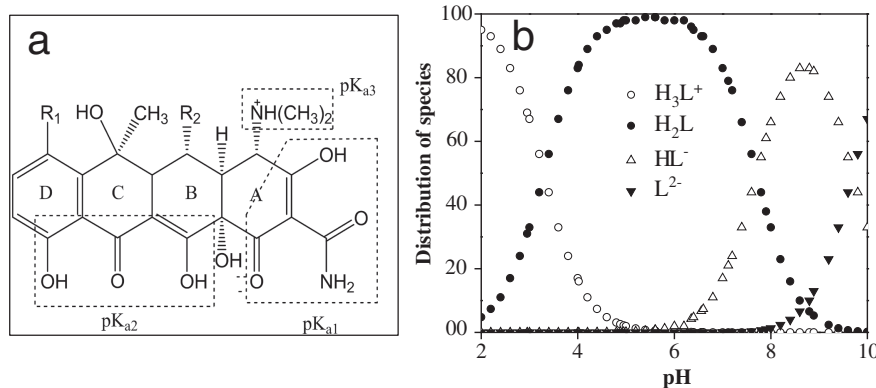


Fig. 7 – The molecular structure of TC (a) and distribution as a function of solution pH (b). TC: tetracycline.

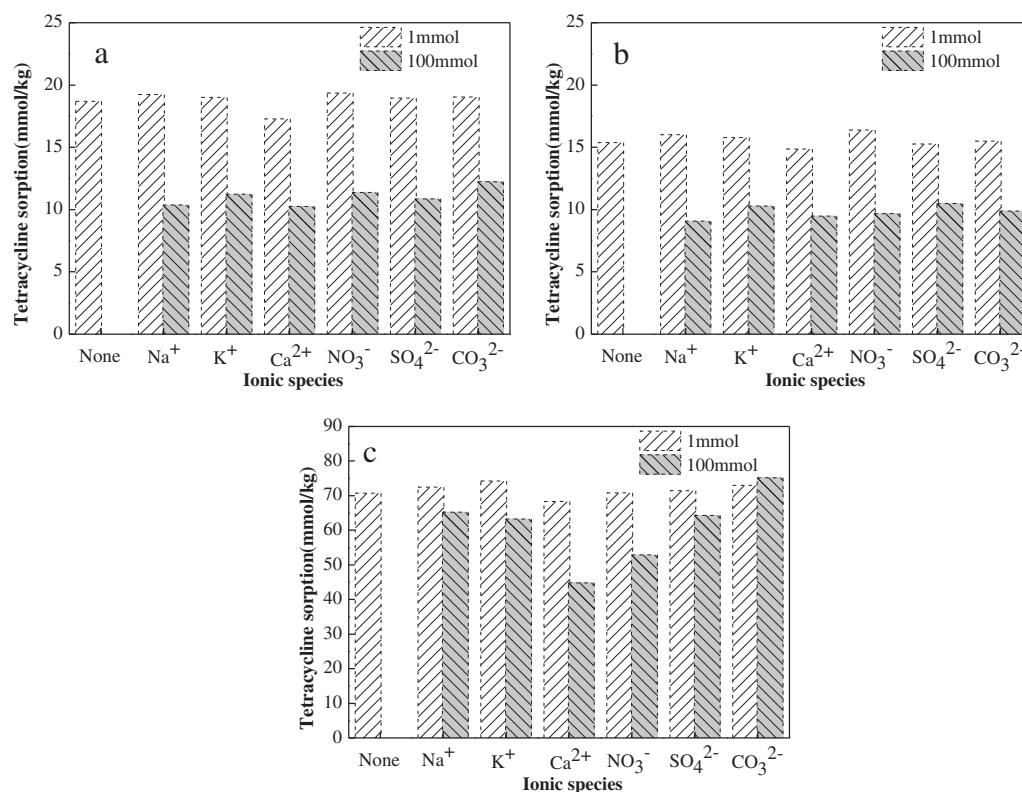


Fig. 8 – The Effect of ionic strength and ion species on the adsorption of TC. (a) SBA15; (b) N3; (c) FeN3. Experimental conditions: [TC]₀ = 0.1 mmol/L, *m* = 1 g/L, pH = 5.0 ± 0.1, *T* = 25°C.

strength increased from 1 to 100 mmol/L, most of adsorption capacity nearly unchanged except Ca²⁺ and CO₃²⁺. It has been reported that inner-sphere complexes are hardly influenced by changes in ionic strength, where outer-sphere complexes are greatly influenced. Hence, the adsorption of TC on SBA15 and N,N-SBA15 may be related to the formation of outer-sphere surface complexes between adsorbate and adsorbent, while the adsorption of TC onto Fe-N,N-SBA15 was mainly attributed to the inner-sphere surface complexes.

3. Conclusions

An adsorbent with multi-functional amino groups and coordinated Fe³⁺ based on mesoporous silica SBA15 was prepared. The influence of amino and Fe³⁺ groups on the surface of mesoporous silica and adsorption behavior was investigated. The results showed that the amino groups could decrease the adsorption capacity of TC while the incorporation of Fe³⁺ could enhance the adsorption process. Furthermore, the solution pH affected the adsorption of TC onto N,N-SBA15 slightly while influenced the adsorption onto Fe-N,N-SBA15 significantly. With the content of Fe³⁺ increased, the adsorption capacity of TC increased. The adsorption kinetics of TC fit pseudo-second-order model well and the equilibrium is achieved in 5 hr. The adsorption isotherms fit the Langmuir model well and the adsorption of TC onto the sorbents was favorable. The ion species has little effect on the adsorption TC onto the adsorbents. The different effects caused by ionic strength were attributed to inner or outer-sphere surface complexes. Overall,

the adsorbents are excellent for antibiotics removal and useful to prepare other materials for environmental applications.

Acknowledgments

This work was supported by Beijing Postdoctoral Science Foundation (No. 21009916007) and Beijing Outstanding Talent Project for Excellent Youth Team (No. 2015000026833T0000). The authors are also grateful to the National Science Fund for Distinguished Young Scholars of China (No. 51225805) and Natural Science Foundation of China (No. 51678025).

REFERENCES

- Ahmed, M.B.A., Zhou, J.L., Ngo, H.H., Guo, W.S., 2015. Adsorptive removal of antibiotics from water and wastewater: progress and challenges. *Sci. Total Environ.* 532, 112–126.
- Alvarez-Torrellas, S., Rodriguez, A., Ovejero, G., 2016. Comparative adsorption performance of ibuprofen and tetracycline from aqueous solution by carbonaceous materials. *Chem. Eng. J.* 283, 936–947.
- Bui, T.X., Choi, H., 2009. Adsorptive removal of selected pharmaceuticals by mesoporous silica SBA-15. *J. Hazard. Mater.* 168 (2–3), 602–608.
- Chang, B.V., Ren, Y.L., 2015. Biodegradation of three tetracyclines in river sediment. *Ecol. Eng.* 75, 272–277.
- Chee-Sanford, J.C., Aminov, R.I., Krapac, I.J., Garrigues-Jeanjean, H., Mackie, R.I., 2001. Occurrence and diversity of tetracycline resistance genes in lagoons and groundwater underlying two

- swine production facilities. *Appl. Environ. Microbiol.* 67 (4), 1494–1502.
- Chen, K., Zhou, J.L., 2014. Occurrence and behavior of antibiotics in water and sediments from the Huangpu River, Shanghai, China. *Chemosphere* 95, 604–612.
- Chen, C.Q., Li, J., Chen, P.P., Ding, R., Zhang, P.F., Li, S.Q., 2014. Occurrence of antibiotics and antibiotic resistances in soils from wastewater irrigation areas in Beijing and Tianjin, China. *Environ. Pollut.* 193, 94–101.
- Dai, J.D., Wei, X., Cao, Z.J., Zhou, Z.P., Yu, P., Pan, J.M., et al., 2014. Highly-controllable imprinted polymer nanoshell at the surface of magnetic halloysite nanotubes for selective recognition and rapid adsorption of tetracycline. *RSC Adv.* 4 (16), 7967–7978.
- Figuerola, R.A., Mackay, A.A., 2005. Sorption of oxytetracycline to iron oxides and iron oxide-rich soils. *Environ. Sci. Technol.* 39 (17), 6664–6671.
- Figuerola, R.A., Leonard, A., Mackay, A.A., 2004. Modeling tetracycline antibiotic sorption to clays. *Environ. Sci. Technol.* 38 (2), 476–483.
- Garg, S., Soni, K., Kumaran, G.M., Kumar, M., Gupta, J.L., Sharma, L.D., et al., 2008. Effect of Zr-SBA-15 support on catalytic functionalities of Mo, CoMo, NiMo hydrotreating catalysts. *Catal. Today* 130 (2–4), 302–308.
- Gu, C., Karthikeyan, K.G., Sibley, S.D., Pedersen, J.A., 2007. Complexation of the antibiotic tetracycline with humic acid. *Chemosphere* 66 (8), 1494–1501.
- Ji, L.L., Chen, W., Duan, L., Zhu, D.Q., 2009. Mechanisms for strong adsorption of tetracycline to carbon nanotubes: a comparative study using activated carbon and graphite as adsorbents. *Environ. Sci. Technol.* 43 (7), 2322–2327.
- Kang, J., Liu, H.J., Zheng, Y.M., Qu, J.H., Chen, J.P., 2010. Systematic study of synergistic and antagonistic effects on adsorption of tetracycline and copper onto a chitosan. *J. Colloid Interface Sci.* 344 (1), 117–125.
- Kim, S.H., Shon, H.K., Ngo, H.H., 2010. Adsorption characteristics of antibiotics trimethoprim on powdered and granular activated carbon. *J. Ind. Eng. Chem.* 16 (3), 344–349.
- Lam, K.F., Yeung, K.L., McKay, G., 2007. Selective mesoporous adsorbents for and Cu^{2+} separation. *Microporous Mesoporous Mater.* 100 (1–3), 191–201.
- Luo, Y., Xu, L., Rysz, M., Wang, Y.Q., Zhang, H., Alvarez, P.J.J., 2011. Occurrence and transport of tetracycline, sulfonamide, quinolone, and macrolide antibiotics in the Haihe River Basin, China. *Environ. Sci. Technol.* 45 (5), 1827–1833.
- Lv, J.M., Ma, Y.L., Chang, X., Fan, S.B., 2015. Removal and removing mechanism of tetracycline residue from aqueous solution by using Cu-13X. *Chem. Eng. J.* 273, 247–253.
- Oh, S., Kang, T., Kim, H., Moon, J., Hong, S., Ti, J., 2007. Preparation of novel ceramic membranes modified by mesoporous silica with 3-aminopropyltriethoxysilane (APTES) and its application to Cu^{2+} separation in the aqueous phase. *J. Membr. Sci.* 301 (1–2), 118–125.
- Ötoker, H.M., Akme Mehmet-Balcioğlu, I., 2005. Adsorption and degradation of enrofloxacin, a veterinary antibiotic on natural zeolite. *J. Hazard. Mater.* 122 (3), 251–258.
- Puanngam, M., Unob, F., 2008. Preparation and use of chemically modified MCM-41 and silica gel as selective adsorbents for Hg(II) ions. *J. Hazard. Mater.* 154 (1–3), 578–587.
- Rivera-Jimenez, S.M., Mendez-Gonzalez, S., Hernandez-Maldonado, A., 2010. Metal ($\text{M} = \text{Co}^{2+}$, Ni^{2+} , and Cu^{2+}) grafted mesoporous SBA-15: effect of transition metal incorporation and pH conditions on the adsorption of Naproxen from water. *Microporous Mesoporous Mater.* 132 (3), 470–479.
- Sassman, S.A., Lee, L.S., 2005. Sorption of three tetracyclines by several soils: assessing the role of pH and cation exchange. *Environ. Sci. Technol.* 39 (19), 7452–7459.
- Tang, J., Shi, T.Z., Wu, X.W., Cao, H.Q., Li, X.D., Hua, R.M., 2015. The occurrence and distribution of antibiotics in Lake Chaohu, China: seasonal variation, potential source and risk assessment. *Chemosphere* 122, 154–161.
- Tong, L., Huang, S.B., Wang, Y.X., Liu, H., Li, M.J., 2014. Occurrence of antibiotics in the aquatic environment of Jiangnan Plain, central China. *Sci. Total Environ.* 497, 180–187.
- Vu, B.K., Snisarenko, O., Lee, H.S., Shin, E.W., 2010a. Adsorption of tetracycline on La-impregnated MCM-41 materials. *Environ. Technol.* 31 (3), 233–241.
- Vu, B.K., Shin, E.W., Snisarenko, O., Jeong, W.S., Lee, H.S., 2010b. Removal of the antibiotic tetracycline by Fe-impregnated SBA-15. *Korean J. Chem. Eng.* 27 (1), 116–120.
- Wang, Y., Gao, B.Y., Yue, W.W., Yue, Q.Y., 2007. Adsorption kinetics of nitrate from aqueous solutions onto modified wheat residue. *Colloids Surf. A Physicochem. Eng. Asp.* 308 (1–3), 1–5.
- Wang, H., Yao, H., Sun, P.Z., Pei, J., Li, D.S., Huang, C.H., 2015. Oxidation of tetracycline antibiotics induced by Fe(III) ions without light irradiation. *Chemosphere* 119, 1255–1261.
- Wu, L.Y., Wang, H.J., Lan, H.C., Liu, H.J., Qu, J.H., 2013. Adsorption of Cu(II)-EDTA chelates on tri-ammonium-functionalized mesoporous silica from aqueous solution. *Sep. Purif. Technol.* 117, 118–123.
- Xu, X.R., Li, X.Y., 2010. Sorption and desorption of antibiotic tetracycline on marine sediments. *Chemosphere* 78 (4), 430–436.
- Yu, D.J., Yi, X.L., Ma, Y.F., Yin, B., Zhou, H.L., Li, J., et al., 2009. Effects of administration mode of antibiotics on antibiotic resistance of *Enterococcus faecalis* in aquatic ecosystems. *Chemosphere* 76 (7), 915–920.
- Zazouli, M.A., Susanto, H., Nasser, S., Ulbricht, M., 2009. Influences of solution chemistry and polymeric natural organic matter on the removal of aquatic pharmaceutical residuals by nanofiltration. *Water Res.* 43 (13), 3270–3280.
- Zhang, Z.Y., Liu, H.J., Wu, L.Y., Lan, H.C., Qu, J.H., 2015a. Preparation of amino-Fe(III) functionalized mesoporous silica for synergistic adsorption of tetracycline and copper. *Chemosphere* 138, 625–632.
- Zhang, Z.Y., Lan, H.C., Liu, H.J., Qu, J.H., 2015b. Removal of tetracycline antibiotics from aqueous solution by amino-Fe (III) functionalized SBA15. *Colloids Surf. A Physicochem. Eng. Asp.* 471, 133–138.
- Zhao, D.Y., Feng, J.L., Huo, Q.S., Melosh, N., Fredrickson, G.H., Chmelka, B.F., et al., 1998. Triblock copolymer syntheses of mesoporous silica with periodic 50 to 300 angstrom pores. *Science* 279 (5350), 548–552.
- Zhao, C., Deng, H.P., Li, Y., Liu, Z.Z., 2010. Photodegradation of oxytetracycline in aqueous by 5A and 13X loaded with TiO_2 under UV irradiation. *J. Hazard. Mater.* 176 (1–3), 884–892.
- Zhao, Y.P., Tong, F., Gu, X.Y., Gu, C., Wang, X.R., Zhang, Y., 2014. Insights into tetracycline adsorption onto goethite: experiments and modeling. *Sci. Total Environ.* 470, 19–25.
- Zuo, J.C., Tong, S.R., Yu, X.L., Wu, L.Y., Cao, C.Y., Ge, M.F., et al., 2012. Fe^{3+} and amino functionalized mesoporous silica: preparation, structural analysis and arsenic adsorption. *J. Hazard. Mater.* 235, 336–342.